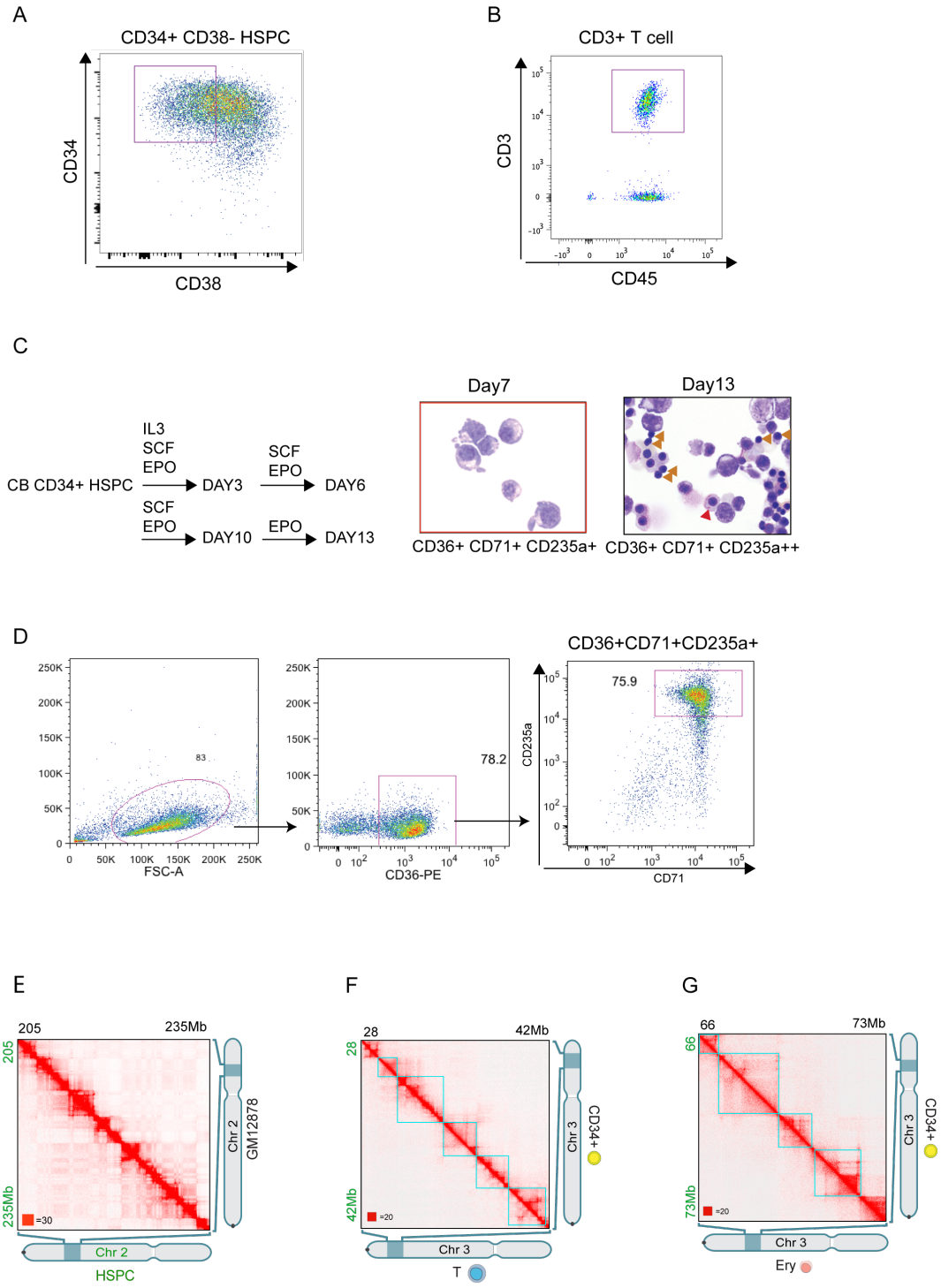

Figure S1. Related to Figure 1. 3D genome of HSPC.

(A) Flow cytometry plot depicting the sorting scheme for the CD34+ CD38– HSPC derived from umbilical cord blood.

(B) The sorting scheme for CD3+ T cells using an anti-CD3 (pan-T-cell) antibody.

(C) The *ex vivo* erythrocyte differentiation procedure. Representative Wright-Giemsa staining of erythroblast populations is shown in the upper panel. The staining of the bulk population is shown in the beginning of *ex vivo* differentiation and Day7/Day13 of *ex vivo* differentiation (lower panel). The brown arrowheads points to the extruded nucleus of erythrocyte on Day13 of *ex vivo* differentiation. The red arrowhead points to erythrocytes with a retained nucleus.

(D) The sorting scheme for erythroblasts on day7 of *ex vivo* differentiation culture.

(E) Typical contact matrix from GM12878 (right) and HSPC (left) chromosome 2 at 25kb resolution.
(F) Contact matrix from HSPCs (right) and T cells (left) chromosome 3 at 25kb resolution.
(G) contact matrix from HSPCs (right) and EPs (left) chromosome 3 at 25kb resolution.

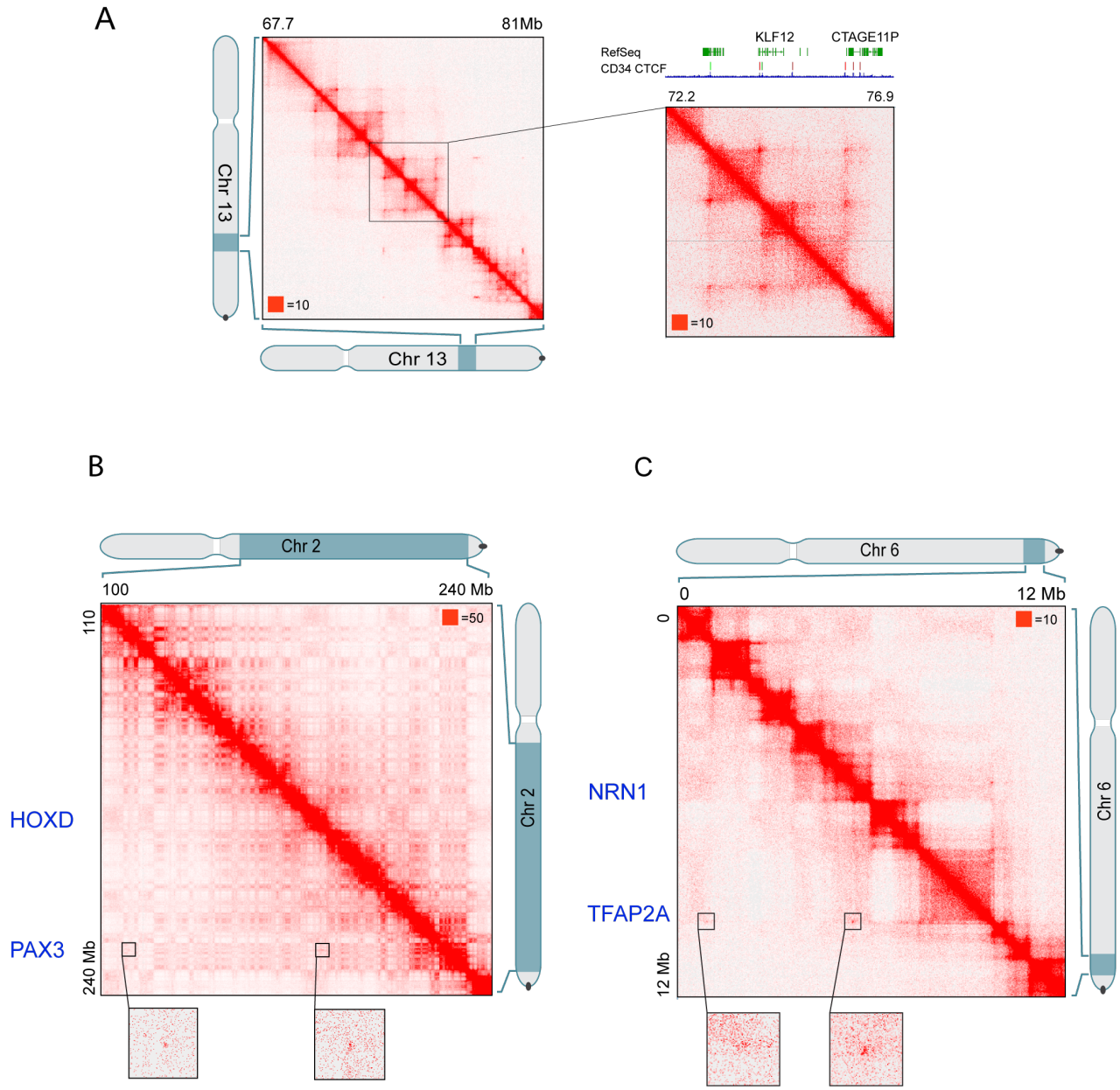

Figure S2. Related to Figure 2. Multiple long-range interactions in the HSPC genome
(A) An example of promoter and enhancer contact loops KLF12 locus from chromosome 13 at 10kb resolution (left) and blowout at 5kb resolution (right).
(B) Example of intra-chromosomal long-range interactions on chromosome 2. The contact map of the *HOXD* and *PAX3* region is shown at shown at 50kb resolution.
(C) Example of intra-chromosomal long-range interactions on chromosome 6. The contact map of the *NRN1* and *TFAP2A* region is shown at shown at 25kb resolution.

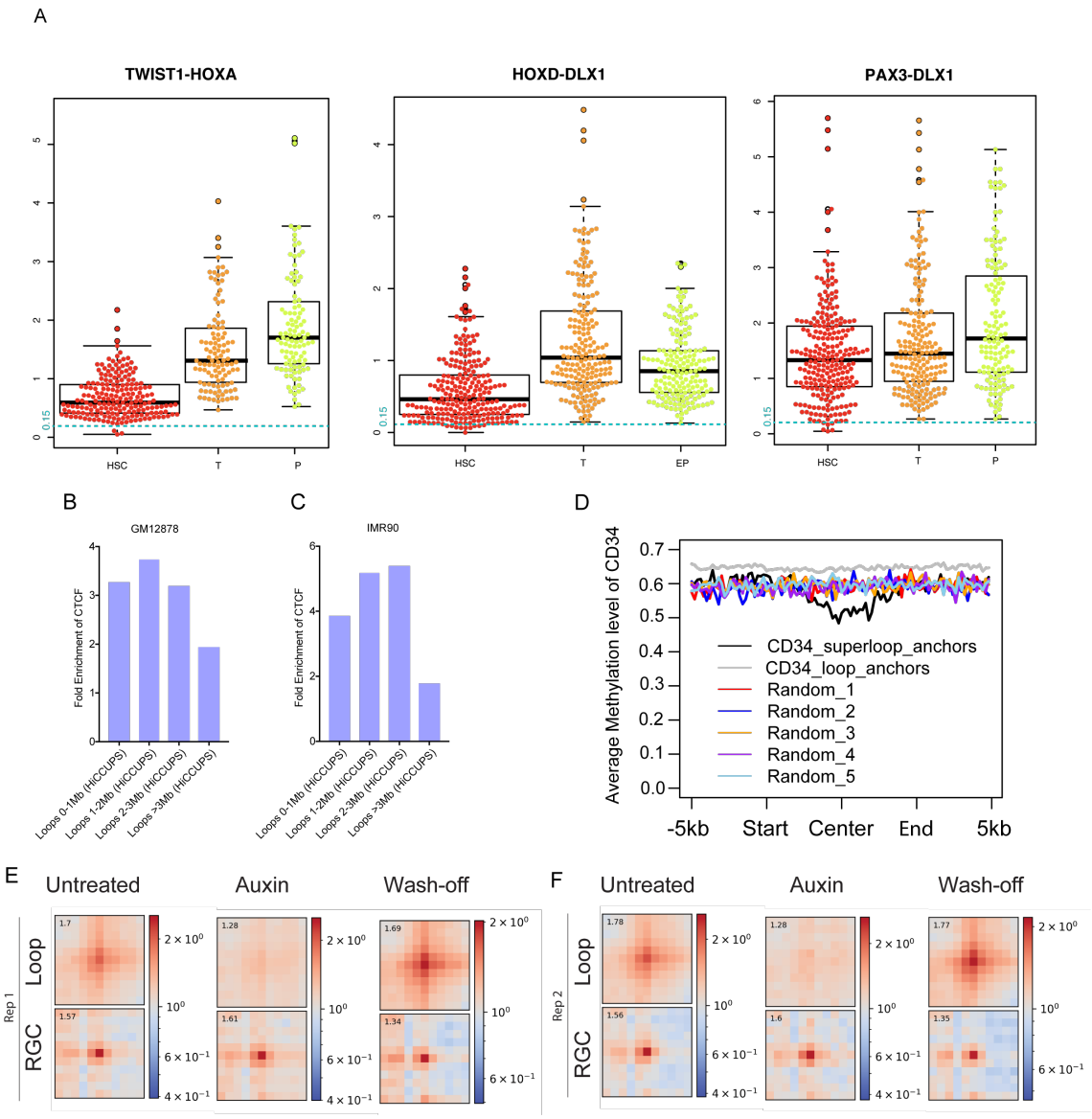

Figure S3. Related to Figure 3 and Figure 4. Enrichment of CTCF and DNA methylation at loop anchors

(A) The distance between *TWIST1-HOXA (p=9.60e-21* HSC vs T*, p=8.96e24* HSC vs EP*), DLX1-HOXD (p=6.42e-23* HSC vs T*, p=7.573-12* HSC vs EP*) and PAX3-DLX1 (p=0.00425* HSC vs T*, p=5.008e-07* HSC vs EP*)* measured by FISH in HSPC (n=120), T cells (n=102) and EPs (n=91). *P* value is calculated by two sample t-test.

(B-C) Fold enrichment of CTCF at loop anchors in GM12878 and (C) IMR90 cells.

(D) DNA methylation level at Long-loop anchors. Average DNA methylation level of HSPC at long loop anchors, loop anchors and random control regions.

(E-F) APA analysis of loop and grand canyon interactions in mouse ES cells. Data from ES cells in which CTCF was degraded with an auxin-inducible degron targeting CTCF (Nora et al. 2017) was analyzed. Analysis of biological duplicates (E and F) are shown separately.

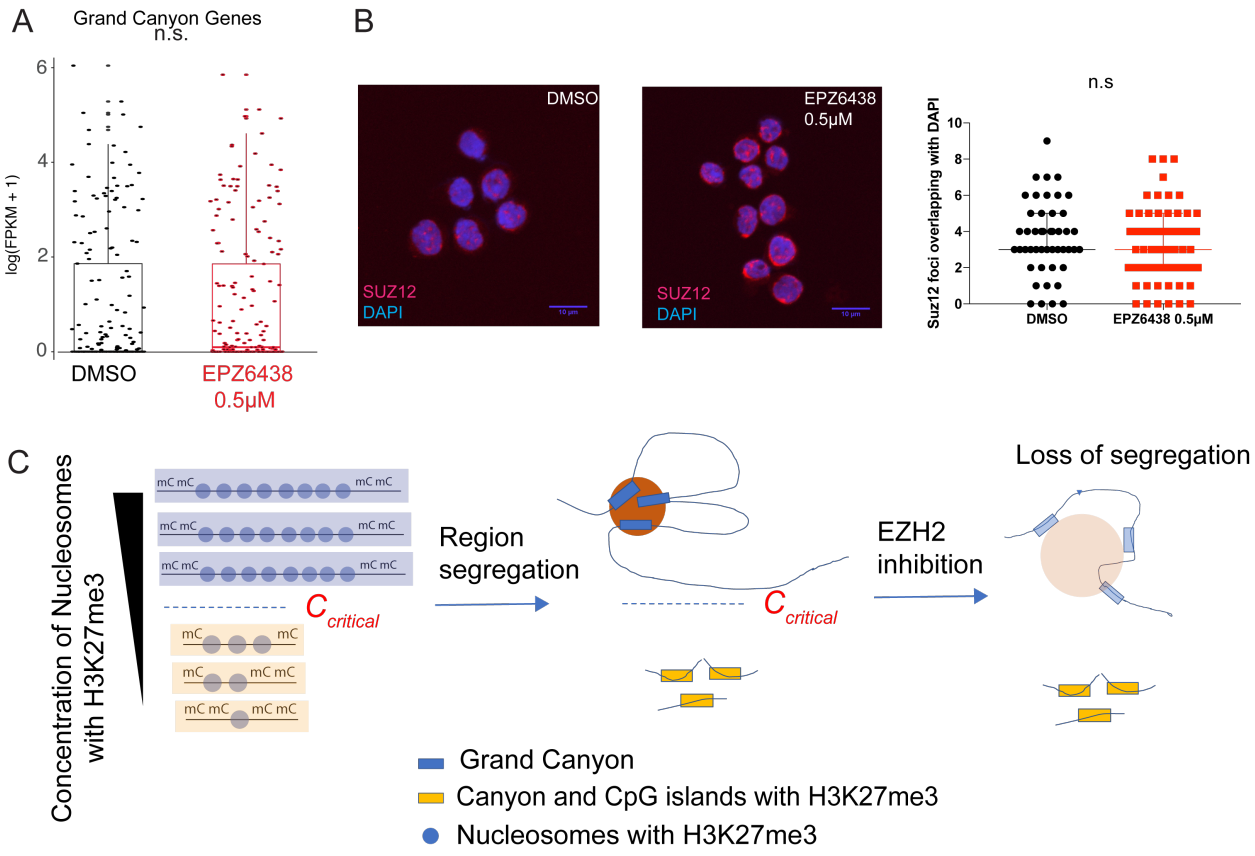

Figure S4. Related to Figure 5. Model for the role of H3K27me3 in grand canyon spatial interactions.
(A) Grand canyon gene expression in DMSO and EPZ6438 treated HSPC. Box plot shows the median and 75 percentile of distribution of log2(FPKM+1). p value is determined by Mann-Whitney test.
(B) Immunofluorescence staining of SUZ12 in DMSO and EPZ6438 treated HSPC. Quantification of SUZ12 foci overlapping with DAPI signal is on the right panel. p value is determined by Student t test.
(C) Model for H3K27me3 in mediating the grand canyon spatial interactions.

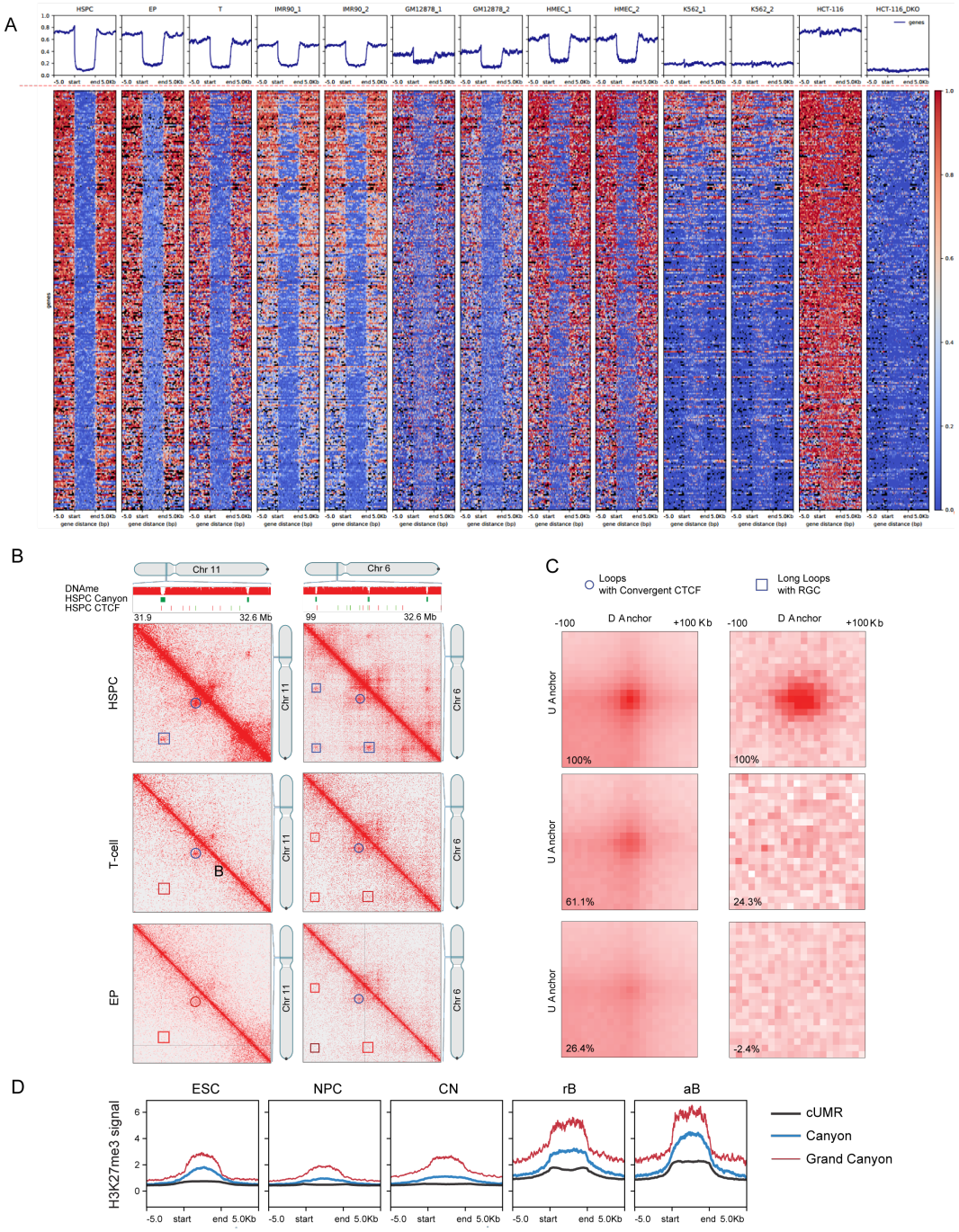

Figure S5. Related to Figure 6 HSPC specific Canyon interactions

(A) DNA methylation heatmap of grand canyons and its flanking regions in cell lines plotted in Figure 6E. Red dotted line indicates grand canyon DNA methylation level in the HSPC.

(B) Example of HiCCUPS loops with convergent CTCF (circles) and loops with repressed grand canyons (squares) on chromosomes 11 and 6 from HSPC, T-cell and EP.

(C) APA analysis of the HSPCs, T-cells and EPs

(D) H3K27me3 enrichment in mouse cells with high resolution HiC data in Figure 6C and Figure S6C.

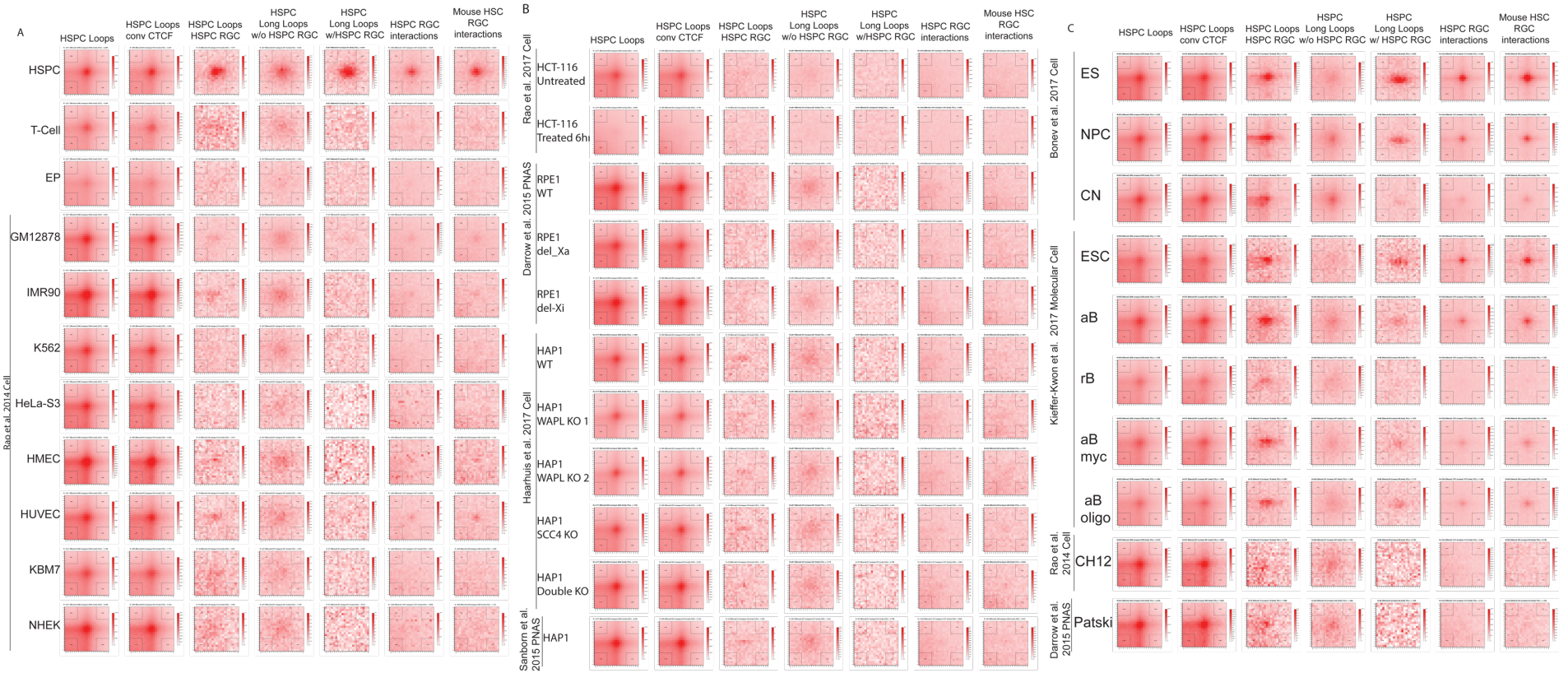
A
HSPC Loops
HSPC Loops conv CTCF
HSPC Loops HSPC RGC
HSPC Long Loops w/o HSPC RGC
HSPC Long Loops w/HSPC RGC
HSPC RGC interactions
Mouse HSC RGC interactions
HSPC
T-Cell
EP
GM12878
IMR90
K562
HeLa-S3
HMEC
HUVEC
KBM7
NHEK
Rao et al. 2014 Cell
B
HCT-116 Untreated
HCT-116 Treated 6h
Rao et al. 2017 Cell
RPE1 WT
RPE1 del_Xa
RPE1 del-Xi
Darrow et al. 2015 PNAS
HAP1 WT
HAP1 WAPL KO 1
HAP1 WAPL KO 2
HAP1 SCC4 KO
HAP1 Double KO
Haarhuis et al. 2017 Cell
HAP1
Sanborn et al. 2015 PNAS
C
ES
NPC
CN
Bonev et al. 2017 Cell
ESC
aB
rB
aB myc
aB oligo
Kieffer-Kwon et al. 2017 Molecular Cell
CH12
Rao et al. 2014 Cell
Patski
Darrow et al. 2015 PNAS

Figure S6. Related to Figure 6. APA Analysis of published human and mouse Hi-C data

(A) APA on HSPC and published human Hi-C data. Each row corresponds to a Hi-C data set. Each column corresponds to APA results from a 2D annotation list. (Left to right: HSPC loops, HSPC loops with convergent CTCF, HSPC loops with HSPC repressive grand canyons, HSPC Long loops without HSPC repressive grand canyons, HSPC Long loops with HSPC repressive grand canyons, pairs of HSPC repressive grand canyons and pairs of mouse HSC repressive grand canyons) The 2D annotation list from mouse cells was liftover from mm9 to hg19 using UCSC liftover tools.

(B) APA on human Hi-C data.

(C) APA on mouse Hi-C data. 2D annotation lists from human cells were liftover from hg19 to mm9 and mm10 using UCSC liftover tools, with the exception that Mouse HSC RGC is obtained from (Jeong et al., 2014).

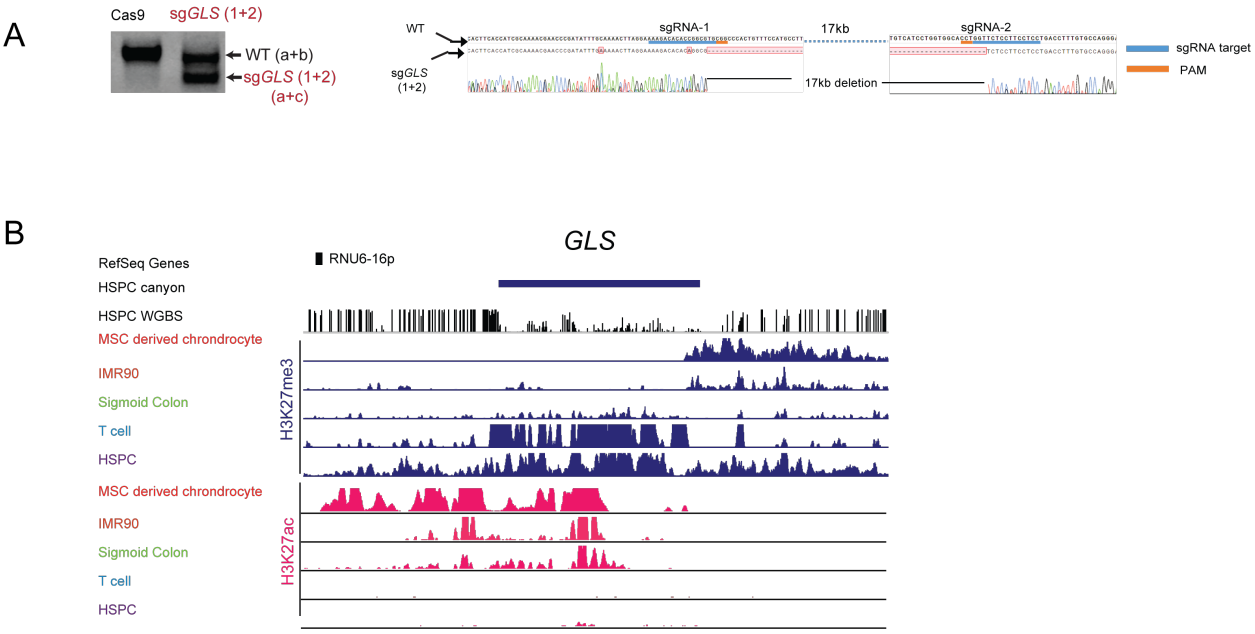

Figure S7. Related to Figure 7. Chromatin status at *GLS* locus in various human cells and tissues.
(A). CRISPR deletion of *GLS* and Sanger Sequencing validation of *GLS* deletion band
(B). The H3K27ac and H3K27me3 distribution in *GLS* locus in different Epigenomics Roadmap cells and tissues.